Field, temperature, and frequency dependence of the surface impedance of $YBa_2Cu_3O_7$ thin films

J. R. Powell and A. Porch
Superconductivity Research Group, The University of Birmingham, Edgbaston, Birmingham, B15 2TT, United Kingdom

R. G. Humphreys
Defence Research Agency, Malvern, Worcestershire, WR14 3PS, United Kingdom

F. Wellhöfer, M. J. Lancaster, and C. E. Gough
Superconductivity Research Group, The University of Birmingham, Edgbaston, Birmingham, B15 2TT, United Kingdom

(Received 28 July 1997)

Measurements of the complex microwave surface impedance of $YBa_2Cu_3O_7$ (YBCO) thin films in a coplanar resonator geometry are reported for a number of films as a function of temperature and field at 8 and 16 GHz. Values are derived for the temperature and field dependence of the Labusch pinning parameter κ_p and for the temperature dependence of η, which are consistent with an independent flux-line model with only weak interflux-line interactions. The observation of losses in the mixed state scaling as $\sim\omega^{1.2}$ and of an effective pinning potential $U\sim 6k_BT$ are shown to be consistent with a glassy-state model, with flux lines thermally activated between local pinning sites separated by energy barriers with a wide range of values extending down to meV energies. The induced curvature of flux lines between point pinning centers is shown to be unimportant in determining the observed microwave properties.
[S0163-1829(98)00605-5]

I. INTRODUCTION

Microwave measurements on high-T_c superconductors in a magnetic field probe the intrinsic dynamics and pinning of flux lines by defects, helping to elucidate properties of intrinsic theoretical interest in addition to those that affect the performance of microwave devices. Coffey-Clem[1] have developed a self-consistent mean-field theory for the electromagnetic properties of flux lines (or bundles) moving in a periodic pinning potential under the combined influence of the induced electromagnetic currents and thermal fluctuations. The model also includes contributions to the losses and field penetration from quasiparticles thermally excited across the energy gap. At low temperatures, when contributions from the thermally activated quasiparticles can be neglected (at least for an *s*-state superconductor) and where flux lines are largely localized close to the minimum of a periodic pinning potential, the Coffey-Clem model reduces to a rather simpler form introduced by Brandt,[2] which highlights the different frequency dependences in the microwave losses expected from intrinsic damping and induced thermal activation of flux lines between pinning centers.

Flux-line dynamics of high-temperature superconductors in the mixed state have been investigated by measurements of the complex microwave surface impedance using a variety of techniques.[3–8] The majority of such measurements have been confined to a single frequency, from which it is not possible to distinguish between viscous damping and thermal depinning of flux lines, which lead to different characteristic frequency-dependent losses. If thermal activation is ignored, the low-frequency losses are expected to vary as ω^2, whereas thermal activation losses do not vary with frequency. Our measurements and previous measurements by Belk *et al.*[9] and Revanez *et al.*[10] suggest a frequency dependence close to $\omega^{1.2}$. Belk *et al.* and Revanez *et al.* interpret their measurements in terms of a glassy-state model with thermal activation of flux lines between a range of closely spaced metastable states as discussed by Koshelev and Vinokur (KV).[11] We adopt a similar analysis and, in agreement with Belk *et al.*, deduce a distribution of pinning energies for the trapped flux lines that extends to very low energies. Assuming such a model, the microwave losses associated with the thermally induced transitions probe the distribution of available energy states on an energy scale of order k_BT.

Deviations from the frequency dependence of the microwave losses predicted from the mean-field theory could, in principle, also arise from the frequency-dependent spatial bending of flux lines between point pinning centers (at the surface or in the bulk) associated with a finite line tension, as considered by Sonin, Tagantsev, and Traito.[12] Such a model makes specific predictions for the frequency dependence of both the real and imaginary parts of the surface impedance, which we consider in Appendix A. If the distribution of distances between pinning centers along the length of a flux line is appropriately chosen, it would, in principle, be possible to model frequency-dependent losses proportional to ω^β over a range of frequencies with any value of β between 0 and 2.

Mean-field theories, in which flux lines are treated independently, like the Coffey-Clem and Brandt models, fail to describe flux-line dynamics at low frequencies, where the combination of flux-line interactions, thermal fluctuations, and local pinning leads to a liquid-glass transition. The properties can then be described by scaling arguments leading to an infinitely large dc-conductivity at small currents.[13] In contrast to low-frequency measurements, there is little evidence for any major change in the temperature or field dependence of microwave penetration or losses on passing across the liquid-glass transition for YBCO thin films and single

crystals.[14] However, Booth, Wu, and Anlage[15] have observed a crossover in frequency dependence from a mean-field to a scaling model below ~ 10 GHz for temperatures above 80 K in YBCO thin-film samples. The lack of any significant changes in microwave properties on passing through the liquid-glass transition in other microwave measurements on YBCO single crystals[14] suggests that an independent flux line rather than a collective motion scaling model analysis is appropriate for analyzing our measurements.

In this paper we present detailed measurements of the field and temperature dependence of the complex microwave surface impedance for a number of epitaxial thin films grown by electron-beam coevaporation, sputtering, and laser ablation. Measurements have been made using a coplanar filter technique at 8 and 16 GHz. Such measurements enable both the penetration depth and microwave losses[16] to be determined absolutely and allow us to separate contributions to the microwave properties from the viscous damping and thermal depinning.

II. THEORETICAL MODELS

The Coffey-Clem (CC) theory describes the ac response of viscously damped flux lines moving in a periodic pinning potential $U\cos(2\pi x/d)$ subject to the microwave-current-induced Lorentz force acting on the flux lines; it also self-consistently includes the effects of thermal fluctuations. The problem is closely related to the ac response of an ionic conductor in a periodic potential, which was solved using the method of continued fractions.[17] CC truncate solutions to first order to reproduce the Ambegaokar-Halperin result[18] for the dc response of a viscously damped particle moving in a periodic potential, leading to a dc mobility $\mu_n I_0(U/k_BT)$, where μ_n is the mobility in the absence of pinning and I_0 is a zero-order Bessel function of the first kind. CC also take into account contributions to the dissipation and penetration of microwaves from normal excitations thermally excited across the gap. The ac response is essentially determined by four terms; the viscously damped induced motion of flux lines about pinning centers, the thermal excitation of flux lines between pinning centers, and contributions from the superconducting and thermally excited quasiparticles. The thermally induced quasiparticle term is usually negligible in comparison to the field-induced terms, other than very close to T_C. CC show that thermal fluctuations not only lead to transitions between pinning centers but also reduce the effective pinning force described by the Labusch parameter κ_p.[19]

At low temperatures ($k_BT \ll U$), thermal fluctuations in the CC model are relatively unimportant and flux lines remain largely localized close to individual minima of the pinning potential, with only occasional thermal activation between pinning centers. The Coffey-Clem predictions then reduce to a rather simple expression introduced by Brandt,[2] in which the complex microwave surface impedance $Z_S = R_S + jX_S = j\mu_0\omega\lambda_{ac}$ can be written as

$$\lambda_{ac}^2 = \lambda_L^2 + \lambda_{fl}^2, \tag{1}$$

where

$$\lambda_{fl} = \lambda_C\left[\frac{1 - j(\omega\tau_0 + 1/\omega\tau_c)}{1+\omega^2\tau_0^2}\right]^{1/2}. \tag{2}$$

In the above expressions, λ_L is the London penetration length, $\lambda_C = (\Phi_0 B/\kappa_p\mu_0)^{1/2}$ is the Campbell penetration depth,[20] and $\tau_0 = \eta/\kappa_p$ is the time constant for the viscously damped motion of flux lines in their individual potential wells. Consistency with the zero-frequency Ambegaokar-Halperin result for thermally activated flux flow resistivity (TAFF) requires that the characteristic time for thermal activation across the pinning barrier $\tau_c = \tau_0 \exp(2U/k_BT)$. We note that the viscous damping and thermally activated creep terms have different frequency dependences. Measurement of the field and frequency dependence of the complex penetration depth, therefore, enables us to derive all the parameters entering Eq. (2).

For an s-state superconductor in zero field, the number of thermally excited normal-state quasiparticles decreases exponentially with temperature and should, therefore, be negligible at low temperatures. However, for a d-state superconductor, the presence of nodes in the gap parameter results in a power-law T dependence at low temperatures. Impurity scattering leads to a broadening of the energy states, a T^2 dependence, and small but finite microwave losses at low temperatures.[21] In practice, the zero-field losses are always significantly larger than predicted by either s- or d-state models. It is therefore usual to add an additional, nonintrinsic, temperature-dependent term $R_0(T)$ to the right-hand side of Eq. (1), which for analysis purposes is assumed to only depend on temperature and frequency. We have also neglected the field dependence expected from the reduction in Cooper pairs in the core of a flux line in a d-state superconductor, which will give rise to a field-dependent $\lambda_L \propto 1/[1-(B/B_{C2})^{1/2}]$[22] giving a curvature in the field dependence of $X_S(B)$ of the opposite sign to that observed.

Two useful limiting forms of Eq. (1) are now given. Changes in the real part of λ_{ac}^2 (which we write as λ_{ac}^2 hereafter) with magnetic field are given by

$$\Delta\lambda_{ac}^2 = \lambda_{fl}^2 = \frac{\Phi_0 B}{\mu_0\kappa_p}\frac{1}{1+\omega^2\tau_0^2}, \tag{3}$$

so that $\Delta\lambda_{ac}^2$ and, in the limit $\Delta X_S \gg \Delta R_S$, ΔX_S^2 should vary linearly with field assuming κ_p to be field independent. Secondly, at low fields when $\lambda_L^2 \gg \lambda_C^2$,

$$Z_S \approx j\mu_0\omega\lambda_L\left[1 + \frac{\lambda_C^2}{2\lambda_L^2}\left(\frac{1 - j(\omega\tau_0 + 1/\omega\tau_C)}{1+\omega^2\tau_0^2}\right)\right]. \tag{4}$$

In this limit, $\Delta R_S/\Delta X_S = \omega\tau_0 + 1/\omega\tau_C$, where $\Delta R_S = R_S(B) - R_S(0)$ and $\Delta X_S = X_S(B) - X_S(0)$. Measurements at more than one frequency are, therefore, required to determine τ_0 and τ_C independently. For self-consistency, the values of τ_0 obtained by this method should also account for the frequency dependence of $\Delta\lambda_{ac}^2$ determined from Eq. (3).

III. EXPERIMENTAL

Microwave measurements were made using coplanar resonator structures lithographically patterned from 350-nm-thick YBCO thin films on (100)MgO substrates. Measure-

TABLE I. Sample numbers, growth techniques, and values for the pinning parameter, κ_p (20 K, $B=0$). δ denotes the deviation of $\Delta\lambda_{ac}^2$ from a linear field dependence where data is fitted using $\Delta\lambda_{ac}^2 \propto B^{1+\delta}$, as in Fig. 3. In the table EB indicates electron-beam coevaporated[24] films; LA, laser ablated,[23] and SP, sputtered.[23]

Sample no.	Growth technique	κ_p (20 K, $B=0$) (10^5 N m^{-2})	δ
1	EB	5.3	0.15
2	LA	2.15	0.28
3	EB	4.5	0.1
4	EB	3.3	0.3
5	EB	3.7	0.1
6	SP	0.9	0.4

ments are reported for a number of films grown by laser ablation,[23] sputtering,[23] and electron-beam coevaporation.[24] Sample numbers and growth techniques are listed in Table I. Patterning was performed by a combination of wet chemical etching and argon ion beam milling to give clean, well-defined edges. Dielectric resonator measurements on the unpatterned films before lithography showed that the subsequent lithography led to no detectable degradation in properties.[25]

Two coplanar resonators were fabricated for each film. The resonators had a 200-μm-wide, 8-mm-long center conductor separated from adjacent ground planes by a 12-μm gap for the ''narrow'' resonator and a 73 μm gap for the ''wide'' resonator. The resonators were mounted in a carefully designed microwave package and placed in a helium continuous flow cryostat enabling measurements to be made from $\sim$6 K to room temperature. The cryostat was mounted in the core of a 6.5 T superconducting magnet with its field perpendicular to the epitaxial ab plane of the thin film. Microwave measurements on the first two coplanar resonator modes at 8 and 16 GHz were made using an HP8722C vector network analyzer. The microwave and measurement system was under computer control, enabling measurements to be made as a function of temperature, field, microwave frequency, and power level. The resolution of the resonant frequency and bandwidth was further improved by signal averaging and computer fitting.

By combining measurements of the changes in the center frequency and bandwidths of the resonances for both the narrow- and wide-gap resonators, absolute values for $\lambda_{ac}(T,B)$ and microwave losses can be extracted, and hence values for R_S and X_S. The method is described elsewhere[16] and is based on the computed current distribution in the thin films as a function of penetration depth and resonator dimensions. The larger concentration of currents flowing near the edges in the narrow resonator leads to a larger kinetic inductance term.

All field measurements were made on heating the sample in a constant applied field after first cooling in the applied field from well above T_C to low temperatures. Such measurements were reversible on thermal cycling within our experimental accuracy (<0.2 K), consistent with the flux in the film remaining uniform and constant. In contrast, measurements in swept fields below $\sim$65 K were always hysteretic, because of magnetic hysteresis and nonuniform penetration of flux.

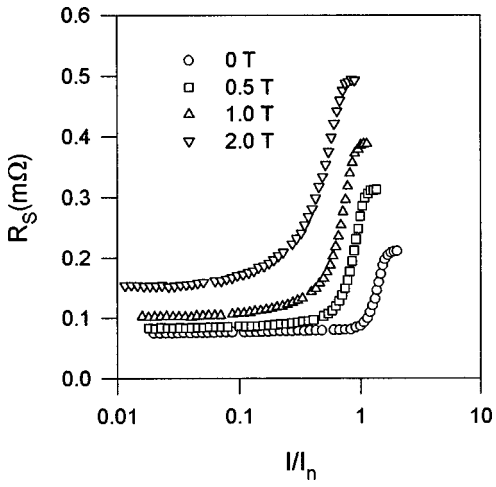

FIG. 1. The onset of nonlinearity in our films illustrated by R_S as a function of peak current flowing at the conductor edge for various applied fields for sample 1 at 15 K. The current is scaled to the current which causes the onset of non-linearity in zero field, which corresponds to a current density $J_n \sim 10$ MA cm^{-2}. These measurements are performed on all films to ensure that our data is taken well within the linear response regime at each applied field.

The microwave response remains linear up to high power levels, see Fig. 1, where the data have been plotted for peak current levels normalized to the peak current required to induce the first indication of nonlinearity in zero field. Experimentally, this was very similar to the measured dc critical current ($\sim 10^7$ A cm^{-2} at low temperatures). This indicates the high quality of the films and patterned edges. All data presented in this paper were obtained at power levels in the linear regime, well below the onset of nonlinearity.

IV. EXPERIMENTAL RESULTS

Examples of the temperature dependence of X_S and R_S extracted from the microwave measurements on an electron-beam coevaporated thin-film (sample 1) coplanar resonator are shown in Fig. 2 for a number of applied fields. Both components of the surface impedance are strongly field and temperature dependent. We note that $R_S \ll X_S$ at all fields and temperatures. Measurements could not be made at higher temperatures because the Q value of the resonators became too low to measure with any accuracy.

In Fig. 3 we have plotted the field dependence of $\Delta\lambda_{ac}^2$ for four samples at several temperatures measured for the fundamental and first-harmonic modes. Although the incremental increase in penetration depth is approximately linear in B, there is significant curvature suggesting that the pinning for these films is weakly field dependent. The solid lines in the figure represent a fit to Eq. (3), where we have included a field-dependent pinning constant giving rise to a change in the penetration depth $\Delta\lambda_{ac}^2 \propto B^{1+\delta}$. Values of δ and $\kappa_p(B=0)$ are included in Table I. Measurements on six different thin films, which included samples grown by electron-beam coevaporation, laser ablation, and sputtering showed a clear correlation between the magnitude of κ_p and the curvature coefficient δ, where the larger the κ_p the more linear the field

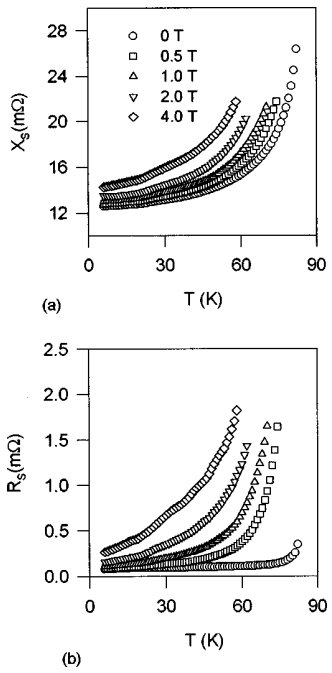

FIG. 2. Typical measurements of the temperature dependence of X_S and R_S extracted from bandwidth and frequency shift measurements plotted for various selected applied fields for the 8 GHz mode of sample 1.

dependence of $\Delta\lambda_{ac}^2$. This is consistent with the deviation in linearity being attributed to weak flux-line interactions, which become more important when the flux lines are only weakly pinned by defects. We also note the slight decrease in $\Delta\lambda_{ac}^2$ with frequency, consistent with the $\omega^2\tau_0^2$ term in the denominator of Eq. (3). By fitting the 8 and 16 GHz data to Eq. (3), we can extract both κ_p and τ_0, and hence the flux-line viscosity $\eta=\kappa_p\tau_0$. Values of κ_p and η for samples 1 and 2 derived in this way from measurements at several temperatures are included as the first three columns of Table II. Similar field and frequency dependences were observed for all six resonator pairs investigated.

TABLE II. Flux line parameters extracted from $\Delta R_S/\Delta X_S$ and $\Delta\lambda_{ac}^2$ data (see text for details) for samples 1 and 2 at various temperatures.

T (K)	κ_p (10^5 N m^{-2})	η (10^{-7} N m^{-2} s)	η/κ_p (ps)	τ_0 (ps)	τ_c (ps)	U (meV)
		Sample 1				
10	6.5	15.0	2.3	0.3	300	6.0
20	5.3	12.2	2.3	0.6	159	9.6
30	4.0	11.6	2.9	0.4	100	14.3
40	3.1	8.4	2.7	0.6	83	17.0
50	2.0	5.8	2.9	0.8	87	20.2
60	1.1	3.2	2.9	1.0	80	22.7
65	0.7	2.7	3.8			
		Sample 2				
10	2.7	6.75	2.5	0.8	174	4.6
20	2.2	5.72	2.6	1.0	110	8.1
30	1.8	5.04	2.8	1.2	99	11.0
40	1.4	3.92	2.8	1.1	77	14.6
50	1.0	2.80	2.8	1.4	73	17.0
60	0.7	2.10	3.0	1.3	66	20.0
65	0.5					

In the absence of thermally activated flux motion, the flux-line contribution to the losses in the strong pinning limit ($X_S \gg R_S$) are expected to scale as ω^2, as in the Meissner state. However, in practice, the losses scale more nearly as

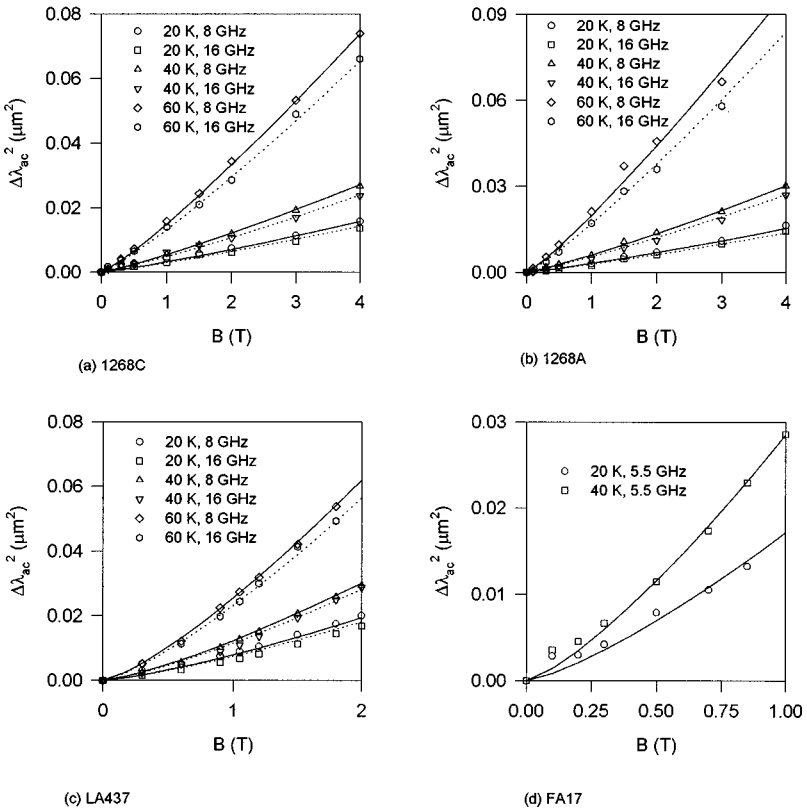

FIG. 3. The field dependence of the change in λ_{ac}^2 as a function of uniformly trapped field at various temperatures for the 8 and 16 GHz modes, plotted for two coevaporated, a laser ablated, and a sputtered film. The curves in the figures are fits to Eq. (3) using the parameters given in Table II.

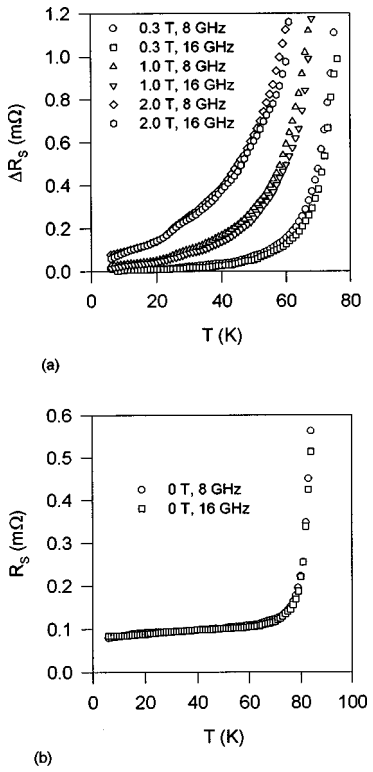

FIG. 4. (a) The temperature dependence of the change in R_S with field for various applied fields, the 16-GHz data is superimposed on that for the 8-GHz mode assuming $\Delta R_S \propto \omega^{1.2}$ scaling at all temperatures. (b) R_S for the 8 and 16 GHz modes in zero applied field. The 16-GHz data is scaled on the 8-GHz mode data assuming $R_S \propto \omega^2$, as expected for these materials.

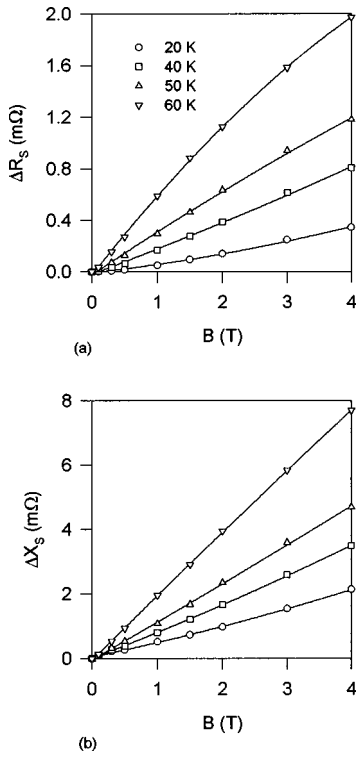

FIG. 5. The change in R_S and X_S as a function of field for various temperatures measured at 8 GHz for sample 2. The lines are simply guides to the eye.

$\omega^{1.2}$, which is the scaling used to overlay the measurements of $\Delta R_S[=R_S(B,T)-R_S(0,T)]$ at 8 and 16 GHz in Fig. 4(a). In zero field, we always observe a rather accurate ω^2 scaling, as illustrated in Fig. 4(b). In the next section we will discuss this scaling for more general models, first involving a random array of pinning centers of variable strength, and secondly, involving a random array of point pinning centers of variable separation along the flux lines.

In Fig. 5, typical measurements of ΔR_S and ΔX_S at 8 GHz are plotted as a function of field for various temperatures. We again note the approximately linear dependence on field. Assuming the idealized Coffey-Clem-Brandt (CCB) model, at low fields, the ratio of these incremental changes gives $\omega\tau_0 + 1/\omega\tau_C$, irrespective of any field dependence of κ_p, as indicated by Eq. (4). To extract τ_0 and τ_C from such measurements, we require data at more than one frequency. The values derived from measurements at 8 and 16 GHz are tabulated in columns 4 and 5 of Table II. Using these values we can extract an effective pinning potential $U(T)$ from the ratio $\tau_C/\tau_0 = \exp(U/k_BT)$, as listed in column 6 of Table II. We find that $U \sim 6k_BT$ for both samples, consistent with earlier measurements of Belk *et al.*[9]

We note from Fig. 5 that ΔX_S is rather accurately proportional to B, whereas ΔR_S shows significant curvature. The apparent linearity in ΔX_S is fortuitous resulting from a cancellation of the upward curvature of $\lambda_{\rm fl}^2$ illustrated in Fig. 3, which occurs inside the expression for the surface impedance from $j\mu_0\omega(\lambda_L^2+\lambda_{\rm fl}^2)^{1/2}$. However, this cannot account for the downward curvature in ΔR_S, which also involves the relaxation times τ_0 and $\tau_C = \tau_0 \exp(U/k_BT)$. The additional curvature almost certainly arises from a field dependence of the pinning potential $U(B,T)$. At higher temperatures and fields, the additional field penetration due to the presence of flux lines becomes comparable or greater than λ_L, as illustrated for sample 1 in Fig. 6, so that higher order terms in the expansion of Eq. (1) become more important.

V. DISCUSSION

The conventional analysis above, based on a periodic, single-valued, potential well depth, enables us to extract the temperature dependences of the three key flux pinning parameters, κ_p, η, and U, and the field dependence of κ_p. We note a variation in values of κ_p and η between samples of about a factor 2, with their ratio remaining approximately

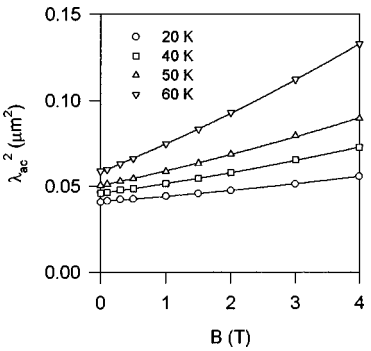

FIG. 6. Field dependence of the derived flux line penetration depth $\lambda_{\rm ac}^2 = \lambda_L^2 + \lambda_{\rm fl}^2$ for sample 1 at various temperatures. At the highest temperatures and fields we note that $\lambda_{\rm fl}^2 \sim \lambda_L^2$.

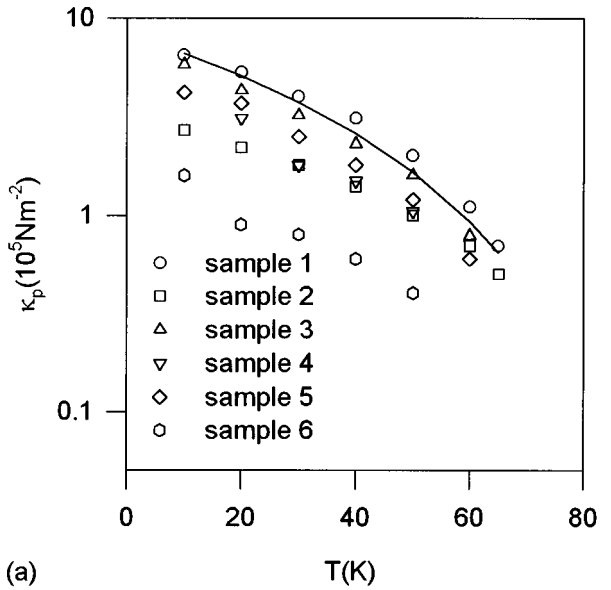

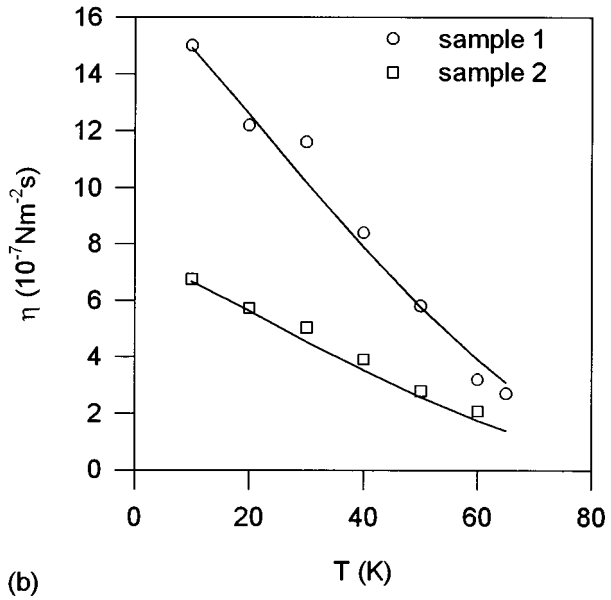

FIG. 7. The temperature dependence of the flux line pinning parameters for various thin-film samples. (a) The flux-line restoring force constant. The solid line in this plot is a fit to the empirical function $\kappa_p=\kappa_{p0}(1-t)^2$, where $t=T/T_C$ and $\kappa_{p0}=8.5\times10^5$ Nm^{-2}. (b) The flux-line viscosity for the two samples for which measurements were made at two frequencies over the full temperature range. The curve in this figure has the form $\eta=\eta_0(1-t)/(1+t^2)$, where $\eta_0=1.7\times10^{-6}$ N s m^{-2} and 7.4×10^{-7} N s m^{-2} for samples 1 and 2, respectively.

constant, as illustrated in Fig. 7.

Previous authors have assumed an empirical expression for the temperature dependence of κ_p based on the pinning energy, related to the condensation energy proportional to H_C^2. Assuming $H_C\propto(1-t^2)$, we would expect $\kappa_p\sim\kappa_{p0}(1-t^2)^2$ in contrast to the observed $\kappa_p\sim\kappa_{p0}(1-t)^2$ corresponding to the solid line drawn through the results in Fig. 7(a). The experimental data, therefore, imply $H_C\sim(1-t)$ at low temperatures. Other authors have suggested that the observed linear temperature dependence arises from thermal fluctuations reducing the effective pinning potential.[8]

Within the framework of the Bardeen-Stephen (BS) theory,[26] the flux line viscosity can be related to the normal-state resistivity ρ_n using

$$\eta=\frac{B_{C2}\Phi_0}{\rho_n}=ne\omega_{C2}\tau_{\rm qp}\Phi_0, \tag{5}$$

where n and $\tau_{\rm qp}$ are the quasiparticle concentration and scattering time, respectively, and $\omega_{C2}=(eB_{c2}/m)$ is the cyclotron frequency at B_{C2} (e and m are the electron charge and mass, respectively). Taking B_{C2} to vary as $B_{C2}\sim(1-t^2)/(1+t^2)$ and $\rho_n\sim1+t$, we obtain the empirical expression $\eta\sim(1-t)/(1+t^2)$, which provides a good description of the data as illustrated by the solid line in Fig. 7(b). However, Eq. (5) assumes the ''dirty limit,'' which may not be appropriate if the separation of localized quasiparticle energy levels in the flux line core is large compared to their uncertainty (i.e., $\omega_{c2}\tau_{\rm qp}\gg1$). Taking $n=5\times10^{27}$ m^{-3} based on ~0.5 carriers per unit cell and η derived in these measurements, we estimate $\omega_{C2}\tau_{\rm qp}$ to be of order unity, as pointed out by Golosovsky for thin films of similar quality.[8] For a conventional s-wave superconductor, this would imply a freezing out of the ''normal-state'' core excitations when $k_BT<h\omega_{C2}\sim100$ K. However, in our measurements (Fig. 2) there is no evidence for any such reduction from normal core contributions down to 6 K. For d-wave superconductivity we can expect a low-lying density of states down to the lowest energies because of the existence of nodal lines of the energy gap function on the Fermi surface.[21] Additional residual losses may also arise from low-lying electronic states associated with defects in the material. However, only states associated with flux lines are likely to account for the linear field dependence shown in Fig. 5(a).

Although we can use the CCB model to derive values for κ_p and η, there are some serious inconsistencies in this analysis. First, we have already noted that the flux-line contribution to the losses at low frequencies are approximately linear in frequency at all temperatures, whereas for a uniformly periodic pinning potential, thermal activation would be negligible at low temperatures, leading to an ω^2 temperature dependence. Furthermore, we obtain a temperature-dependent effective pinning strength $U\sim6k_BT$, which is again incompatible with the CCB models. Comparing columns 4 and 5 in Table II, we also see that the value of the viscous drag damping time constant τ_0 derived from $\Delta\lambda_{\rm ac}^2$ is significantly larger than the value derived from $\Delta R_S/\Delta X_S$, whereas they should be identical within the periodic, single-valued, potential-well model. Finally, since we expect κ_p to be proportional to $\partial^2U/\partial x^2$, both κ_p and U should have similar temperature dependences, whereas they vary with temperature in opposite senses.

To account for the above discrepencies, we must, therefore, introduce a more sophisticated model for the pinning of flux lines in a high-T_C superconductor. We consider two models, first assuming a random array of pinning centers with a wide distribution of pinning energy U extending to very low energies, initially proposed by Koshelev and Vinokur[11] and applied to microwave measurements by Belk *et al.*[9]; second, we consider the effect of a finite line tension leading to a bowing out of the flux lines between point pinning centers distributed at random along the length of the

flux lines, which is closely related to models introduced earlier by Sonin, Tagantsev, and Traito.[12]

Flux lines in high-T_C superconductors are generally believed to undergo a liquid-to-glass structural phase transition, which for the fields used in these experiments (up to 4 T) occurs above 85 K. Hence all the measurements reported here were well within the vortex glass state, where the dc resistivity becomes vanishingly small at low currents. However, in typical measurements at microwave frequencies, with induced current densities $J<10^5$ A cm^{-2}, flux lines do move, but only over very small distances ($\sim$few Å) about their equilibrium positions. There is then significant dissipation associated with viscous damping and thermal activation over pinning barriers. Our measurements imply that the thermal activation of flux lines between pinning sites of closely spaced energies, as discussed by Koshelev and Vinokur (KV),[11] remains important down to low temperatures.

The KV model assumes that the flux lines are close to thermal equilibrium in a random array of pinning centers of variable strengths. When the thermal equilibrium distribution is perturbed by the microwave current, the flux lines make transitions across the intervening energy barriers to the new thermal equilibrium distribution, with a time constant $\tau_{th} \sim \tau_a \exp(U/k_BT)$, where τ_a is an effective attempt time. Such relaxation will be dominated by flux lines moving across energy barriers $\sim O(k_BT)$ or less in magnitude. Measurement of the losses associated with the equilibration of the thermal equilibrium distribution, therefore, provides information about the local distribution of pinning barrier heights $g(U)$. An effective pinning potential $U\sim 6k_BT$ can be described if we invoke a uniform distribution of pinning barriers extending to very small energies $<k_BT$. These low-lying energy barriers may well involve changes in configurational states, involving only slight changes in the correlated positions of the flux lines in the presence of a relatively high density background of local pinning centers. When the barriers from localized defects become sufficiently small, one would indeed anticipate interactions between the flux lines themselves to become important. This is also consistent with the small field dependence deduced for κ_p.

Belk *et al.*[9] derived an expression for the ac susceptibility for such a model, which we express in terms of $\lambda_{\rm fl}$ as

$$\lambda_{\rm fl}^2=\frac{\Phi_0 B}{\mu_0}\left[\frac{d^2 l}{4k_BT}\int_0^\infty \frac{g(U)dU}{1+j\omega\tau_a\exp(U/k_BT)}+\frac{1/\kappa_p}{1+j\omega\tau_0}\right], \tag{6}$$

where flux lines of length l are assumed to be able to make thermal hopping transitions over a barrier height U to a new pinning center at a distance d. Note that the standard CCB model for a uniformly periodic pinning potential can be recovered if we take $g(U)=\delta(U-U_P)/U_P$ and set $d^2 l k_P/4U_P=\tau_a/\tau_0$. If instead we assume a constant density of pinning energies $g(U)=1/U_P$, the integral in the above expression has the analytic solution $(k_BT/U_0)\ln(1+1/j\omega\tau_a)$, so that in the limit $\omega\tau_a\ll 1$ we may write

$$\lambda_{\rm fl}^2=\frac{\Phi_0 B}{\mu_0}\left[\frac{d^2 l}{4Up}\left(-\frac{\pi}{2}j-\ln(\omega\tau_a)\right)+\frac{1/\kappa_p}{1+j\omega\tau_0}\right]. \tag{7}$$

Note that the imaginary term arising from thermal fluctuations is constant and independent of frequency, implying microwave losses proportional to frequency, similar to that observed. If such losses had been interpreted within the CCB model, an effective pinning energy $U^*=k_BT\ln(8U_P/\pi d^2 l\kappa_p\omega\tau_a)$ would have been derived, which only depends weakly on frequency. If $\tau_a\sim\tau_0\sim 10^{-12}$ s, $\omega\tau_a\sim 0.1$ at 10 GHz. From experiment $U^*\sim 6k_BT$, so that $U_P/d^2 l\kappa_p\sim 16$. An even more realistic model would have also taken into account the expected distribution in the unknown values of d and l. However, since these parameters appear within the logarithmic term, this would not affect the result significantly.

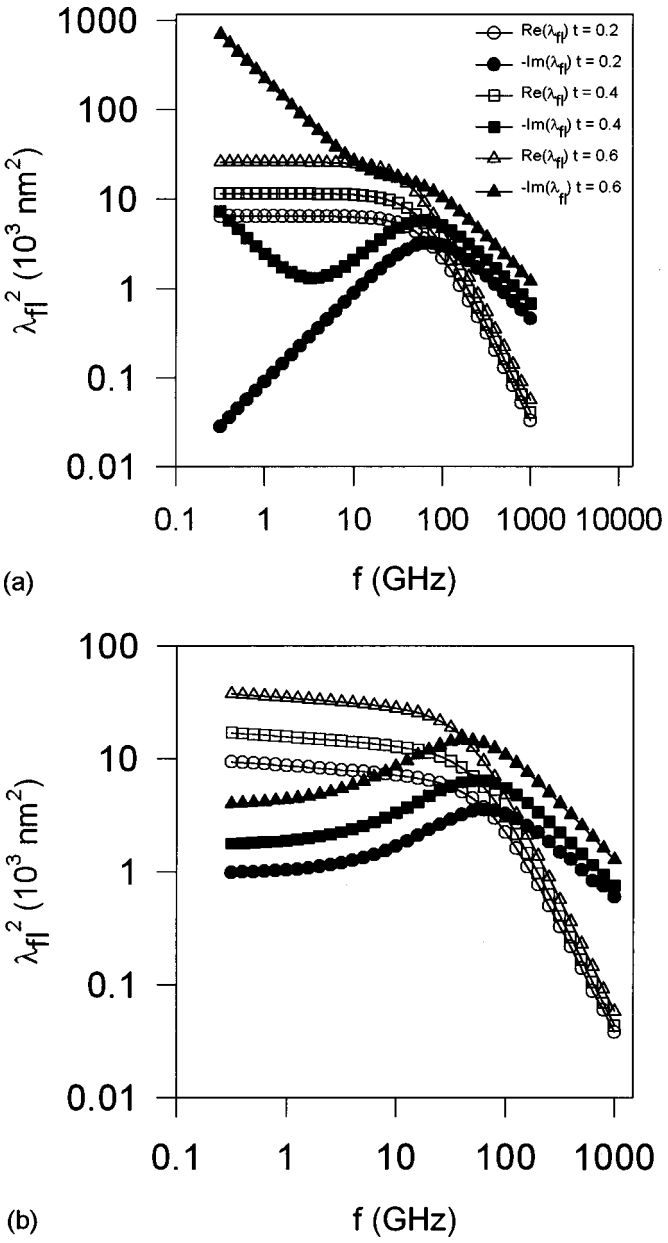

FIG. 8. The frequency dependence of the real and imaginary parts of the flux-line penetration depth $\lambda_{\rm fl}$ using (a) the single potential well model, and (b) a distribution of potential wells as described in the text.

In Figs. 8(a) and 8(b) we contrast the frequency dependence for $\lambda_{\rm fl}^2$ predicted by the CCB model of a flux line moving in a uniformly periodic pinning potential, with that predicted by the KV glassy-state model as described above.

In plotting these data we have used the experimentally derived values for κ_p and η giving $\tau_0 \sim 2$ ps, and have set $U_P/d^2 l k_p = 16$, so that at 10 GHz we obtain $U^* \sim 6 k_B T$. For consistency with our experimental data we find that we also have to use the expression $g(U) = (1 + U_P/U_0)/U_0$ identical to that used by Belk *et al.*[9] The plots then show the expected constancy of the imaginary component at low frequencies corresponding to the nearly linear frequency dependence of losses in qualitative agreement with the $\omega^{1.2}$ dependence deduced from our results and those of Belk *et al.*[9]

All the models discussed above assume either that flux lines move as rigid rods between pinning centers or that the pinning is uniformly distributed along their length. However, as the flux lines have a finite (rather than infinite) line tension T, the Lorentz force along their length will force them to bend between pinning centers giving an additional displacement and hence an additional contribution to the surface reactance and losses. The consequences of such motions on the dynamics of flux motion have been considered previously by Sonin, Tagantsev, and Traito.[12] The line tension for an isolated flux line T can be identified with $c_{44}^{\rm corr} \cong \Phi_0^2/4\pi\mu_0\lambda_C^2 \ln \Gamma\kappa$, derived by Sudbo and Brandt,[27] where we can assume the large $\Gamma\kappa$ limit, where Γ is the anisotropy factor and κ is the kappa value for currents flowing in the ab plane. If, as we will justify later, the induced microwave currents vary slowly compared with the distance d between pinning centers, it is straightforward to show, in Appendix A, that

$$\lambda_{\rm fl}^2 = \frac{\Phi_0 B}{j\mu_0\omega\eta}\left[\frac{[1 - f(\omega/\omega_0)] + j(\omega/\omega_p) f(\omega/\omega_0)}{1 + j(\omega/\omega_p) f(\omega/\omega_0)}\right]. \quad (8)$$

The pinning frequency $\omega_p = K/\eta d$, where K (equivalent to $\kappa_p d$ in the CCB models) is the force constant at the localized point pinning centers, $\omega_0 = T/\eta d^2$ and $f(\omega/\omega_0) = \tanh(\sqrt{j\omega/\omega_0})/\sqrt{j\omega/\omega_0}$. At low frequencies the mean flux-line displacement is $\Phi_0 J/\kappa_p[1 + \omega_p/3\omega_0]$, while at high frequencies the displacement is $\Phi_0 J/j\omega\eta$ and is uniform along most of the length and is dominated by viscous damping.

In Fig. 9(a) we have plotted the frequency dependence of the real and imaginary components of $\lambda_{\rm fl}^2$ as a function of ω/ω_p for various values of ω_p/ω_0. The Coffey-Clem-Brandt model corresponds to large T and hence to vanishingly small ω_p/ω_0. The effect of a non-negligible line tension is to increase the average displacement at low frequencies by the factor $(1 + \omega_p/3\omega_0)$ and to decrease the crossover frequency between the ω and $1/\omega$ dependences at low and high frequencies. From the frequency dependence alone, it would be very difficult to distinguish between this model and models assuming uniform pinning along the length of the flux lines.

In our experiments, the distance between pinning centers cannot exceed the film thickness ~ 300 nm. For this distance the crossover frequency would be ~ 10 MHz, where we have taken $\eta \sim 10^{-6}$ N m^{-2} s from experiment and have estimated $T \sim 10^{-12}$ N m^{-2} assuming values for $\lambda_C \sim 1$ μm. Such a low crossover frequency would imply $\Delta R_S(B) = \Delta X_S(B)$, whereas we observe $\Delta R_S(B) \ll \Delta X_S(B)$ and losses varying $\sim\omega$. The crossover frequency must, therefore, be considerably greater than 10 GHz, implying a distance between pinning centers of $\leqslant 10$ nm (several unit cells along the c direction).

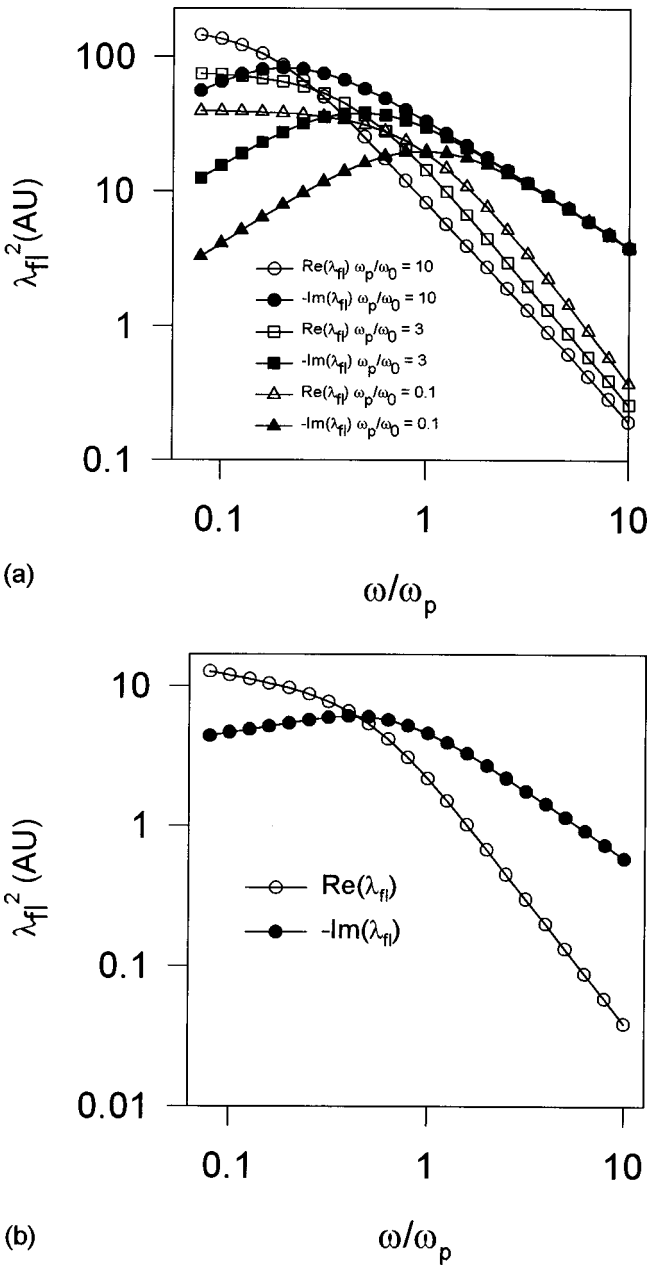

FIG. 9. The frequency dependence of the real and imaginary parts of the flux-line penetration depth $\lambda_{\rm fl}$. In (a) $\lambda_{\rm fl}$ is plotted using the point pinning model for various values of the ω_0/ω_p. (b) $\lambda_{\rm fl}$ is plotted for a weighted distribution of values of $\omega_0/\omega_p = 0.1$, 0.5, and 3 with weighting factors 0.3, 0.7, and 1. Giving a frequency dependence below ω_p qualitatively consistent with our measurements.

The flexible flux-line model could also describe the observed quasilinear dependence of the flux contribution to the losses on frequency, if we assume an appropriate distribution of distances between pinning centers. This is illustrated in Fig. 9(b), where we have considered contributions from flux lines with three pinning lengths, with the longer lengths preferentially weighted. We have adjusted the parameters to give a similar value for $\Delta R_S(B)/\Delta X_S(B)$ to that observed in our experiments (~ 0.3).

Although we can describe the quasilinear frequency dependence of the losses either by a distribution in the energies of pinning centers or by a finite line tension with a distribution in spacing between the pinning centers, the observation of an effective activation energy $U \sim 6k_BT$ argues strongly in terms of the first interpretation. Nevertheless, the second model is still relevant because it enables us to put an upper limit on the distance between pinning centers of the order 10 unit cells or less.

VI. CONCLUSIONS

Using a pair of coplanar linear resonators patterned on the same film, we have been able to deduce absolute values for the field- and temperature-dependent penetration lengths and microwave losses for a number of thin films deposited by laser ablation, sputtering, and electron-beam coevaporation at 8 and 16 GHz. The field and frequency dependences of the microwave properties of these films were all very similar.

The measurements were first analyzed in terms of the CCB models, which are based on a highly simplified model of flux lines uniformly pinned along their length by a periodic pinning potential. We emphasize that measurements at more than one frequency are necessary to extract information on both the viscous damping and thermal creep losses. This remains true even at the lowest temperatures measured, where thermally activated losses appear to remain significant, leading to an effective pinning energy $\sim 6k_BT$. Our measurements exhibit incremental changes in both surface reactance and resistance varying approximately linearly with field at small fields. This justifies the use of an independent flux line (mean-field) model, though small deviations from linearity at larger fields suggest the increasing importance of interactions between flux lines. We note that we have neglected any field dependence of λ_L that may arise from nodes in the energy gap in a d-state superconductor, which would give curvature in the field dependence of $X_S(B)$ in the opposite sense to that observed.

Values of κ_p and η extracted from the initial field and the frequency dependence of the inductive component are similar to those extracted from the measured ratio $\Delta R_S/\Delta X_S$ at a single frequency by other authors.[3–8] However, by measuring the losses at more than one frequency, we have demonstrated that thermally activated flux loss effects are important at all temperatures and fields studied, so that reliable measurements of the bulk pinning and damping cannot be made from measurements at a single frequency.

However, there are serious inconsistencies in the interpretation of the data using the CCB models. Most importantly, the losses in a magnetic field exhibit a quasilinear rather than quadratic frequency dependence, similar to earlier observations by Belk *et al.*[9] The pinning potential deduced from the CCB model was found to depend linearly with temperature with $U \sim 6k_BT$, at variance with the idea of typical pinning potentials with energies ~ 100 meV deduced from creep measurements.[28]

To account for these discrepancies, we have followed Belk *et al.*[9] and have analyzed our measurements in terms of a model of distributed pinning barriers first introduced by Koshelev and Vinokur.[11] We show that both the nearly linear frequency dependence and the temperature-dependent effective pinning potential can be successfully described by such a model using reasonable values for the fitting parameters assumed. We have also considered the effect of a finite line tension leading to bending of flux lines between point pinning centers. In all our measurements $\Delta R_S(B)/\Delta X_S(B) \ll 1$, so that elastic pinning must always remain more important than viscous damping. This enables us to put an upper limit on the distance between the point pinning centers along the length of the flux lines of $\sim 1/30$ of the film thickness (i.e., ~ 10 nm or less). This short distance between pinning centers justifies the model that we have been using for microwave losses, where we assume that the flux dynamics is determined on a local scale, much smaller than the distance over which the microwave currents vary significantly.

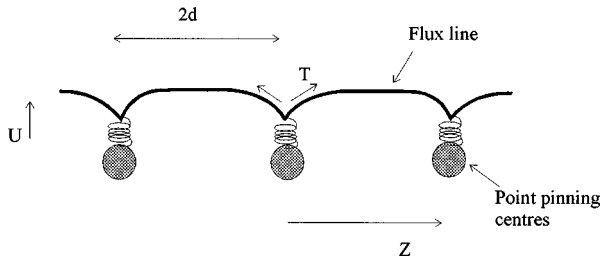

FIG. 10. A schematic diagram of a flux line held at point pinning centers. The flux line can be displaced from its equilibrium pinning position at the pins and will bow out between pinning centers by an amount that depends on the line tension.

In conclusion, our measurements imply that the dynamics of flux lines in the mixed state of a high-temperature superconductor is significantly more complicated than described by the conventional Coffey-Clem and Brandt models. To account for the observed temperature and frequency dependence of the microwave penetration and losses, it is necessary to invoke a wide range of pinning energies and barriers to thermal motion extending to energies <1 meV, almost two orders of magnitude lower than the pinning energies typically derived from creep measurements.[28] Creep involves the large scale collective motion of flux lines, whereas the microwave properties are largely determined by the small-scale motion ($\leqslant 1$ Å) about the assumed point pinning centers.

Such motions may well be affected by quite small changes in configurational energy of the flux line assembly as nearby flux lines are thermally activated. Since quantum tunneling is believed to be a dominant flux creep mechanism at low temperatures,[29] it would be surprising if quantum tunneling was not also important in determining the microwave response at low temperatures. This would lead to temperature-independent losses in the presence of a magnetic field at low temperatures.

ACKNOWLEDGMENTS

This research was supported by the EPSRC under the University of Birmingham Superconductivity Programme (Grant No. GR/J85523). We thank Eduard Sonin for helpful discussions and Gary Walsh for his expect technical support.

APPENDIX A: THE FLUX-LINE SURFACE IMPEDANCE IN THE PRESENCE OF POINT PINNING CENTERS

The CCB models for flux dynamics effectively assume either uniform pinning along the length of a flux line, or

point pinning along the length with a sufficiently large line tension so that the flux lines move as rigid rods between pinning centers. Here, we present a model for flux lines that have a finite line tension. The flux lines are pinned at localized points along their length, and bow out between them, as illustrated for a regular array of pinning centers in Fig. 10.

The flux-line displacements at and between the pinning centers are determined by the restoring force constant K at the pinning centers and the effective line tension T, which has been derived by Sudbo and Brandt,[27] who obtain

$$T = c_{44}^{\mathrm{corr}} = \frac{1}{4\pi\mu_0}\left(\frac{\Phi_0}{\lambda_C}\right)^2 \ln\tilde{\kappa},$$

where

$$\tilde{\kappa}^2 = \frac{1+\Gamma^2\kappa^2+k_z^2\lambda_{ab}^2}{1+\Gamma^2\kappa^2(B/B_{c2})+k_z^2\lambda_{ab}^2}.$$

Γ is the anisotropy factor, $\kappa=\lambda_{ab}/\xi_{ab}$, and k_z is the Fourier component of the transverse line displacements. To a very good approximation, at sufficiently small fields, and in the large $\Gamma\kappa$ limit, $\tilde{\kappa}=\Gamma\kappa$. We also note that any dependence on k_z is very small other than in the extreme limit when $k_z\lambda_{ab} \gg 1$, so that we do not need to take into account any effects due to a finite rigidity or quasidiscontinuous changes in slope of flux lines near the pinning centers themselves.

The dynamics of flux lines of finite line tension has been treated by Sonin, Tagantzev, and Traito,[12] who considered the general case when variations in the microwave currents occur on a similar length scale to the characteristic diffusion length $\sim(T/\omega\eta)^{1/2}$ for propagating transverse displacements of the flux line. In our experimental configuration, the applied field is perpendicular to the film, and the microwave currents are approximately constant across the width of the thin film. We can, therefore, assume a uniformly distributed Lorentz force $\sim\Phi_0 J$ along the length of the flux lines, which simplifies the analysis. The equation of motion can then be written as

$$\eta\frac{\partial u}{\partial t} = \Phi_0 J + T\frac{\partial^2 u}{\partial z^2},$$

where u is the transverse flux-line displacement. This has solutions of the form

$$u = \Phi_0 J/j\omega\eta + A\cosh(kz), \tag{A1}$$

where $k=(j\omega\eta/T)^{1/2}$ is the inverse diffusion length. For point pinning at $\pm d$,

$$T\left(\frac{\partial u}{\partial z}\right)_{z=\pm d} = -Ku, \tag{A2}$$

where $K=2\kappa_p d$. Using Eqs. (A1) and (A2), we then arrive at the following expression for the flux-line displacement:

$$u(z) = \frac{\Phi_0 J}{j\omega\eta}\left[-\frac{1}{1+\frac{Tk}{K}\tanh(kd)}\frac{\cosh(kz)}{\cosh(kd)}\right]. \tag{A3}$$

Averaging over the length of the flux line gives the mean flux-line displacement,

$$u_{\mathrm{av}} = \frac{\Phi_0 J}{j\omega\eta}\left[\frac{K\left[1-\frac{\tanh(kd)}{kd}\right]+j\omega\eta d\,\frac{\tanh(kd)}{kd}}{K+j\omega\eta d\,\frac{\tanh(kd)}{kd}}\right]. \tag{A4}$$

We can then introduce a scaling frequency $\omega_0=T/\eta d^2$, which enables us to rewrite Eq. (A4) in the form

$$u_{\mathrm{av}} = \frac{\Phi_0 J}{j\omega\eta}\left(\frac{K[1-f(\omega/\omega_0)]+j\omega\eta d f(\omega/\omega_0)}{K+j\omega\eta d f(\omega/\omega_0)}\right), \tag{A5}$$

where

$$f(\omega/\omega_0) = \frac{\tanh(j\omega/\omega_0)^{1/2}}{(j\omega/\omega_0)^{1/2}}.$$

This reduces to the CCB result when $\omega_p \ll \omega_0$, where $\omega_p = K/\eta d$. In the limit $\omega\to 0$, $u_{\mathrm{av}}=(\Phi_0 J/K)(I+\omega_p/3\omega_0)$, and when $\omega\to\infty$ $u_{\mathrm{av}}=\Phi_0 J/j\omega\eta$.

The above result can be used to modify the standard CCB expression by incorporating the modified expression for u_{av}. This results in a complex penetration depth given by

$$\lambda_{\mathrm{ac}} = (\lambda_L^2+\lambda_{\mathrm{fl}}^2)^{1/2},$$

where

$$\lambda_{\mathrm{fl}}^2 = \frac{Bu_{\mathrm{av}}}{\mu_0 J}.$$

J is the microwave driving current and u_{av} is given by Eq. (A5). The real and imaginary components of λ_{fl}^2 for this model are plotted in Fig. 9 for a number of different values of ω_p/ω_0.

[1] M. W. Coffey and J. R. Clem, Phys. Rev. Lett. **67**, 386 (1991).

[2] E. H. Brandt, Phys. Rev. Lett. **67**, 2219 (1991).

[3] I. S. Ghosh, L. F. Cohen, V. Fry, T. Tate, A. D. Caplin, J. Gallop, S. Sievers, R. Somekh, S. Hensen, and M. Lenkens, IEEE Trans. Appl. Supercond. **5**, 1756 (1995).

[4] N. Anand and M. Tinkham, Phys. Rev. B **52**, 3784 (1995).

[5] M. S. Pambianchi, D. H. Wu, L. Ganapathi, and S. M. Anlage, IEEE Trans. Appl. Supercond. **3**, 2774 (1993).

[6] Y. Matsuda, N. P. Ong, Y. F. Yan, J. M. Harris, and J. B. Peterson, Phys. Rev. B **49**, 4380 (1994).

[7] J. Owliaei and S. Sridhar, Phys. Rev. Lett. **69**, 3366 (1992).

[8] M. Golosovsky, M. Tsindlekht, and D. Davidson, Supercond. Sci. Technol. **9**, 1 (1996).

[9] N. Belk, D. E. Oates, D. A. Feld, G. Dresselhaus, and M. S. Dresselhaus, Phys. Rev. B **53**, 3459 (1996).

[10] S. Revenaz, D. E. Oates, D. Labrelavigne, G. Dresselhaus, and M. S. Dresselhaus, Phys. Rev. B **50**, 118 (1994).

[11] A. E. Koshelev and V. M. Vinokur, Physica C **173**, 465 (1991).

[12] E. B. Sonin, A. K. Tagantsev, and K. B. Traito, Phys. Rev. B **46**, 5830 (1992).
[13] D. S. Fisher, M. P. A. Fisher, and D. A. Huse, Phys. Rev. B **43**, 130 (1991).
[14] N. J. Exon, A. Porch, M. J. Lancaster, and C. E. Gough, Physica B **194**, 1603 (1994).
[15] D. H. Wu, J. C. Booth, and S. M. Anlage, Phys. Rev. Lett. **75**, 525 (1995).
[16] A. Porch, M. J. Lancaster, and R. G. Humphreys, IEEE Trans. Microwave Theory Tech. **43**, 306 (1995).
[17] P. Fulde, Phys. Rev. Lett. **35**, 1776 (1971).
[18] V. Ambegaokar and B. I. Halperin, Phys. Rev. Lett. **22**, 1364 (1969).
[19] R. Labusch, Cryst. Lattice Defects **1**, (1969).
[20] A. M. Campbell, J. Phys. C **4**, 3186 (1971).
[21] P. J. Hirschfeld, W. O. Putikka, and D. J. Scalapino, Phys. Rev. Lett. **71**, 3705 (1993).
[22] S. K. Yip and J. A. Sauls, Phys. Rev. Lett. **69**, 2264 (1992).
[23] B. Avenhaus *et al.*, IEEE Trans. Appl. Supercond. **5**, 1737 (1995).
[24] N. G. Chew, S. W. Goodyear, J. A. Edwards, J. A. Satchell, S. E. Blenkisop, and R. G. Humphreys, Appl. Phys. Lett. **57**, 2016 (1990).
[25] A. Porch, B. Avenhaus, F. Wellhöfer, and P. Woodall, in *Proceedings of the European Applied Superconductivity Conference*, edited by D. Dew-Hughes, IOP Conf. Proc. No. 148 (Institute of Physics and Physical Society, London, 1995), p. 1039.
[26] J. Bardeen and M. H. Stephen, Phys. Rev. **140**, A1197 (1965).
[27] A. Sudbo and E. H. Brandt, Phys. Rev. Lett. **66**, 1781 (1991).
[28] R. Griessen, J. G. Lensink, and H. G. Schnack, Physica C **185**,337 (1991).
[29] P. Berghuis, R. Herzog, R. E. Somekh, J. E. Evetts, R. A. Doyle, F. Baudenbacher, and A. M. Campbell, Physica C **256**, 13 (1996).